Letter   **Editors' Suggestion**

Two-step aging dynamics in enzymatic milk gels

Julien Bauland,[1] Gouranga Manna,[2] Thibaut Divoux,[1] and Thomas Gibaud[1,*]

[1]*ENSL, CNRS, Laboratoire de Physique, F-69342 Lyon, France*
[2]*ESRF, The European Synchrotron, Grenoble 38043, France*

Colloidal gels undergo a phenomenon known as physical aging, i.e., a continuous change of their physical properties with time. To date, most of the research effort on aging in gels has been focused on suspensions of hard colloidal particles. In this Letter, we tackle the case of soft colloidal "micelles" comprised of proteins, in which gelation is induced by the addition of an enzyme. Using time-resolved mechanical spectroscopy, we monitor the viscoelastic properties of a suspension of colloidal micelles through the sol-gel transition and subsequent aging. We show that the microscopic scenario underpinning the macroscopic aging dynamics comprises two sequential steps. First, the gel microstructure undergoes rapid coarsening, as observed by optical microscopy, followed by arrest. Second, aging occurs solely through a contact-driven mechanism, as evidenced by the square-root dependence of the yield stress with the elastic modulus measured at different ages of the gel. These results provide a comprehensive understanding of aging in enzymatic milk gels, crucial for a broad range of dairy products, and for soft colloids in general.

Gels are two-component systems, composed of a continuous fluid phase in which a small fraction of dispersed phase, such as polymers, colloids, or droplets, imparts solid-like properties to the dispersion. These soft solids find applications in countless fields, from ensuring the texture of food products [1,2] to tissue engineering [3], and environmental sciences [4].

For particulate colloidal gels, the sol-gel transition results from the formation of a stress-bearing network due to attractive interactions between colloids. The network can be open and fractal or conversely compact and made of glassy strands, depending on the colloid volume fraction and the magnitude of attractive forces with respect to thermal energy [5–9]. The structure and dynamics of the network bear crucial importance in determining the rheological properties of colloidal gels [10–13].

In general, colloidal gels show time-dependent properties referred to as "aging", where the gel elastic modulus increases as a function of time [14–17]. Aging has been attributed to two different microscopic origins. Firstly, it may arise from structural rearrangements, driven by either local reorganizations of the constituents due to thermal agitation [18] or by larger scale or cooperative rearrangements resulting from internal stress relaxation [19–21]. Secondly, a change in colloid interactions with time can lead to aging without any accompanying structural changes [14,22,23].

Here, we focus on enzymatic milk gels formed through enzymatic destabilization of casein "micelles", which are natural colloids composed of proteins and salts. Casein micelles can be likened to microgels with a diameter of about 100 nm, in which thousands of proteins are held together through noncovalent interactions [24–26]. Enzymatic milk gels display

pronounced aging, which is a key feature during the early stages of cheese manufacturing [27,28]. Despite its industrial significance and numerous studies reporting on milk gel rheological properties, the aging mechanisms and their impact on the viscoelastic properties of enzymatic milk gels remain not fully understood [29–31].

In this Letter, we address the aging mechanisms of enzymatic milk gels. Viscoelastic spectrum measured across the sol-gel transition allows us to build a master curve, which shows that enzymatic milk gels, tested at various volume fractions, obey a time-connectivity superposition principle akin to the time-cure superposition principle originally identified in polymer gels [32–34]. Such a continuous evolution in the macroscopic response of enzymatic milk gels is related to extensive rearrangements of the gel microstructure, which lead to an increase of the fractal dimension of the gel network. We then identify a second aging regime, during which the gel elasticity increases solely through a contact-driven mechanism. This behavior is in stark contrast with some gels made of hard colloids, in which the aging scenario does not involve structural rearrangements of the network formed at the gel point [35].

Reconstituted milk was obtained by dispersing a skim milk powder in water to reach a volume fraction of casein micelles ϕ equal to 10%. Volume fractions in the range 5–20% were then prepared from the stock suspension (see the Supplemental Material, SM [36]). Gelation was initiated at 30 °C by adding an enzymatic coagulant, thereby setting the time $t = 0$ s. While still liquid, the suspension was introduced into a double-wall concentric cylinder geometry connected to a strain-controlled rheometer to perform rheological measurements through the sol-gel transition. Linear viscoelastic spectra were measured periodically using multifrequency chirp signals to monitor the rapid temporal evolution of the elastic

---

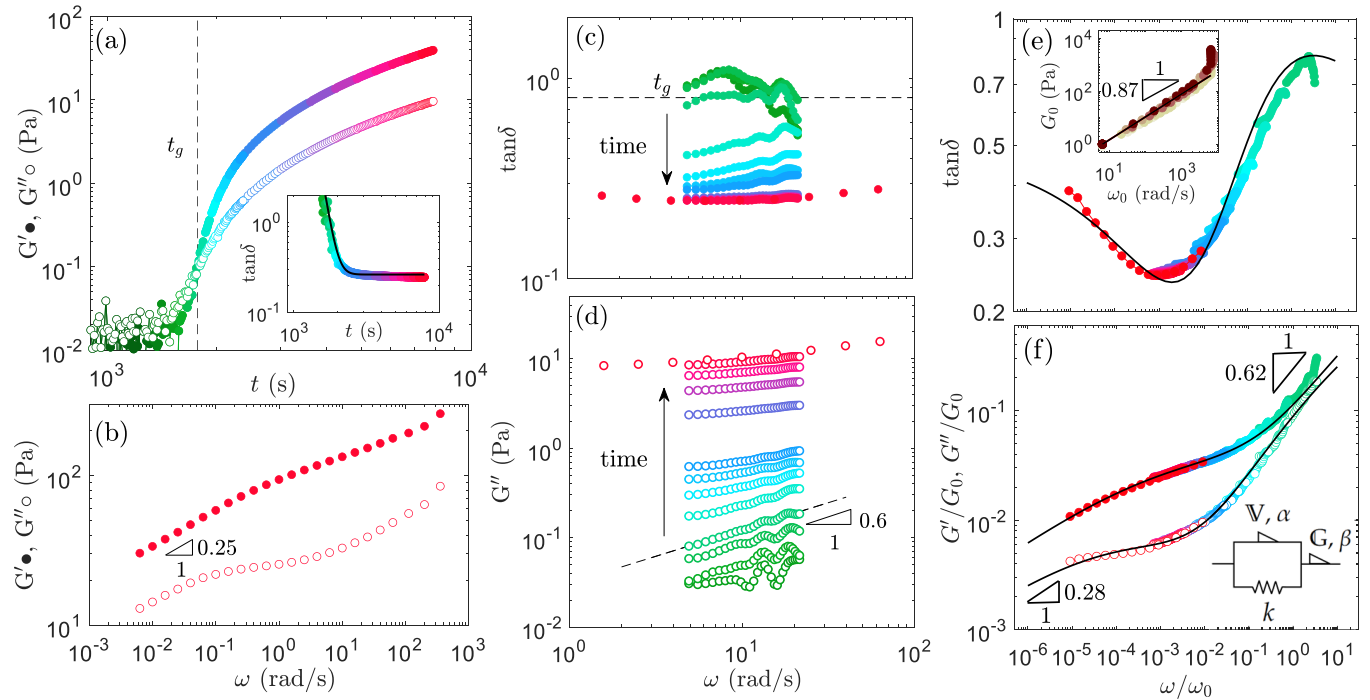*Contact author: thomas.gibaud@ens-lyon.fr

FIG. 1. (a) Temporal evolution of elastic G' and viscous G'' moduli measured at $\omega = 0.628$ rad/s and a strain amplitude of $\gamma = 0.01$ after coagulant addition to the milk suspension at $\phi = 10\%$. The gel time $t_g = 1770$ s is indicated by the black-dotted line. (Inset) $\tan\delta$ vs t fitted by an exponential decay (black line) with τ a characteristic time equals to 150 s. (b) Viscoelastic spectra of mature gel determined at $t = 2 \times 10^4$ s as a function of ω. [(c),(d)] Viscoelastic spectrum obtained from chirp measurements: (c) $\tan\delta$ and (d) G'' vs ω. Colors code for the aging time as depicted in (a). The full viscoelastic spectra of the mature gel is also displayed for comparison (red). [(e),(f)] Evolution of the loss tangent and rescaled moduli as a function of the rescaled angular frequency ω/ω_0. The black curves correspond to the best fit of the data with a fractional Poynting-Thomson model. [Inset in (e)] Scaling factors G_0 vs ω_0 for different ϕ: from light yellow to dark red for $\phi = 5, 7.5, 10, 15,$ and 20%. [Inset in (f)] Drawing of the fractional Poynting-Thomson model.

and viscous moduli (see the SM [36]) [35,37]. In addition to rheological measurements, the sample microstructure was determined by ultra-small-angle x-ray scattering (USAXS), conducted at the European Synchrotron Radiation Facility (ESRF, ID02 beamline, France), and confocal microscopy. At all time scales, all our gel samples adhere to the walls of the measuring cells, whether we used rheology, SAXS, or confocal microscopy. This adhesion prevents the samples from displaying syneresis macroscopically; thus, the samples remain soft, homogeneous solids at the macroscopic level and do not phase separate by expelling the solvent from the gel phase.

We first investigate the gelation kinetics of the suspension with $\phi = 10\%$. In Fig. 1(a), the elastic and viscous moduli G' and G'' quickly increase after a latency period of about 1000 s, which corresponds to the enzymatic destabilization and aggregation of casein micelles [38]. The gel point, defined as the time t_g at which $\tan\delta$ is frequency independent [32,39], is found to be $t_g = 1770$ s. Concurrent to the increase of the moduli, the loss tangent quickly decreases from $\tan\delta > 1$ to about 0.3, following an exponential-like decay $\tan\delta(t) = \exp[(t_g - t)/\tau] + k$, with k the plateau value of $\tan\delta(t)$ at long time and τ, a characteristic time equal to $\tau = 150$ s [inset in Fig. 1(a)].

Using multifrequency chirp signals [35,37], we monitor the rapid evolution of the viscoelastic spectra throughout the sol-gel transition, as displayed in Figs. 1(c) and 1(d). At the critical point t_g, $G'(\omega) \sim G''(\omega) \sim \omega^\beta$, with $\beta = 0.62$

{Fig. 1(d) and Fig. S1(c) within the SM [36]}. This power-law response is linked to the self-similar nature of the percolated network at the gel point, which can be compactly described by its fractal dimension d_f. Beyond the gel point, the viscoelastic spectrum evolves until it coincides with the spectrum of the mature gel obtained from a simple frequency sweep and initiated at $t \sim 2 \times 10^4$ s [Fig. 1(b)].

Inspired by earlier reports on the viscoelastic properties of gels near the gel point [12,35,40–43], a single master curve can be constructed from the continuous evolution of $\tan\delta(\omega)$ by horizontally shifting the curves using a time-dependent scaling factor $\omega_0(t)$ [Fig. 1(e)]. Similarly, $G'(\omega/\omega_0)$ and $G''(\omega/\omega_0)$ can be rescaled by vertically shifting the curves using a second scaling factor $G_0(t)$ [Fig. 1(f)]. The scaling of the viscoelastic spectra acquired at different aging times points to a time-connectivity superposition principle, as reported for polymer [34,44] and particle gels [35,43]. The time-connectivity principle highlights that structural changes taking place during aging essentially result in a change of scale and connectivity while retaining the same self-similar organization.

The master curves G'/G_0 and G''/G_0 vs (ω/ω_0) span over six orders of magnitude and display power laws both in the high- and low-frequency limits. Power-law responses are efficiently captured by fractional models and the introduction of a spring-pot element. Its constitutive equation follows $\sigma = \mathbb{V}d^\alpha\gamma/dt^\alpha$, with α a dimensionless exponent, that interpolates
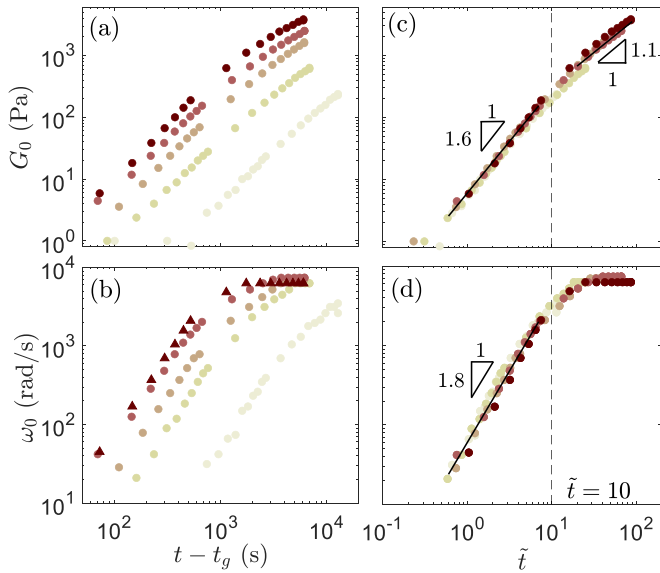
FIG. 2. [(a),(b)] Scaling factors G_0 and ω_0 as function of the elapsed time since the gel point $t - t_g$ at various volume fractions. Colors code for the volume fraction of colloids: from light yellow to dark red $\phi = 5, 7.5, 10, 15$, and 20%. [(c),(d)] G_0 and ω_0 displayed as function of the reduced time $\tilde{t} = (t - t_g)/\tau$, with τ the characteristic time extracted from the exponential decay of $\tan\delta(t)$.

between a spring-like ($\alpha = 0$) and a dashpot-like ($\alpha = 1$) response. Moreover, $\mathbb{V}$ is a "quasiproperty" with dimension Pa.s$^\alpha$ [45–47]. Here, the full viscoelastic spectrum can be captured by a Poynting-Thomson model [46] composed of a spring-pot ($\mathbb{G}, \beta$) in series with a fractional Kelvin-Voigt element ($\mathbb{V}, \alpha$, and k) [sketch in inset of Fig. 1(f)]. By varying the volume fraction of casein micelles, we found that this evolution of the viscoelastic properties is robust for $5 \leqslant \phi \leqslant 20\%$ and that the exponents $\beta = 0.62 \pm 0.04$ and $\alpha = 0.28 \pm 0.01$ are independent of ϕ {Fig. S4(b) within the SM [36]}.

The time dependence of the complete viscoelastic properties is contained in the evolution of the scaling factors $G_0(t)$ and $\omega_0(t)$, the characteristic elasticity and representative time scale of the material, respectively. They are displayed as a function of the reduced time $t - t_g$ in Figs. 2(a) and 2(b) for various volume fractions. All curves $G_0(t - t_g)$ and $\omega_0(t - t_g)$ collapse onto master curves [Figs. 2(c) and 2(d)], when plotted as a function of a dimensionless time $\tilde{t} = (t - t_g)/\tau$, with τ the characteristic time extracted from the exponential decay of $\tan\delta$ with time [inset in Fig. 1(a)]. First, such scaling indicates that, irrespective of the colloid volume fraction, the evolution of the viscoelastic properties of enzymatic milk gels during aging follows the same pathway. As τ decreases with ϕ according to $\tau \propto \phi^{-1.4}$ {Fig. S4(a) within the SM [36]}, only the speed of the aging process increases with ϕ. Second, the evolution of $G_0(\tilde{t})$ and $\omega_0(\tilde{t})$ shows two dynamics, separated by a common transition time $\tilde{t}_c \approx 10$. For $\tilde{t} < \tilde{t}_c$, both G_0 and ω_0 increase as power laws of $\tilde{t}$ with exponents of 1.6 and 1.8, respectively. In contrast, for $\tilde{t} \geqslant \tilde{t}_c$, ω_0 is constant and G_0 increases almost linearly with $\tilde{t}$.

To gain insights into the microscopic mechanisms underlying this two-step aging process separated by $\tilde{t}_c$, we probe the gel structure at $\phi = 10\%$ using USAXS and confocal
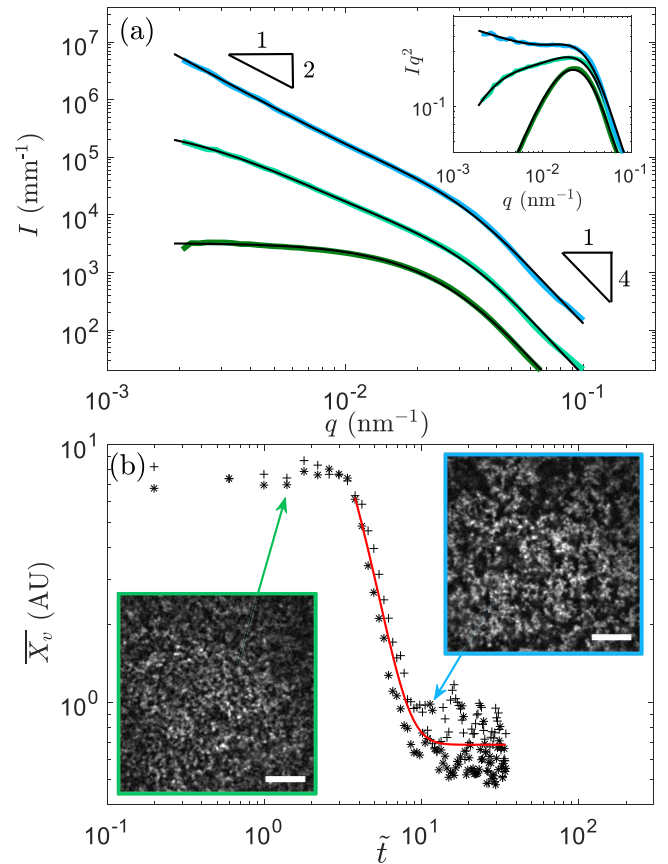

FIG. 3. (a) USAXS intensity $I(q)$ vs the scattering wave vector q at selected aging times, $\tilde{t} = -6, 0$, and 10 from bottom to top. For clarity, the horizontal shift factors equal to 10 and 100 are applied for $\tilde{t} = 0$ and 10, respectively. (Inset) Kratky plot $I.q^2$ vs q. Black lines are fit to the data (see the SM [36]). (b) Magnitude of displacement vectors $\overline{X}_v$ computed by cross correlation of confocal images recorded during the sample aging. $\overline{X}_v$ is taken as an estimate of structural change between two successive images. Red curve represents the best exponential decay fit of the data. (Inset) Confocal images at $\tilde{t} = 0$ and 10. The scale bar represents 10 μm.

microscopy. Figure 3(a) displays the scattered intensity $I(q)$ plotted against the wave vector q. At $\tilde{t} = -6$ (i.e., immediately after coagulant addition), the scattering intensity of the stable casein micelles suspension shows a Guinier plateau at low q attributed to the spherical form factor $P(q)$ of the colloids [48]. As time increases, casein micelles structure into a network of clusters characterized by a fractal dimension d_f which results in a power-law scaling $I(q < 0.02) \sim q^{-d_f}$, that can be captured by a mass fractal structure factor $S(q)$ [49]. At the gel point ($\tilde{t} = 0$), $d_f = 2$ and increases to $d_f = 2.2$ at $\tilde{t} = 10$ [Fig. 3(a)]. This change of fractal dimension during aging, as reflected by a change in $I(q)$, is better visualized when the are displayed using Kratky representation [inset in Fig. 3(a)]. The increase in d_f over time indicates that the percolated network of casein micelles spontaneously coarsens during aging, i.e., the clusters of casein micelles that compose the gel network become denser. We note that we could fit the data at all time scales using $I(q, t) \propto P(q)S(q, t)$, keeping $P(q)$ unchanged. This indicates that the casein micelle form

factor in the tested q range remains unaffected by gelation (see the SM [36]).

To quantify the dynamics of the structural changes occurring at length scales larger than that accessible by X-ray scattering, we monitor the evolution of enzymatic milk gels by confocal microscopy (see Movie 1 within the SM [36]). Casein micelles that appear in white, quickly structure into freely diffusing clusters. These clusters percolate and their dynamics become arrested at a transition time beyond which changes in the microstructure appear local. Using cross-correlation analysis, we track the displacement of the gray-scale structures over successive images using a strategy developed for particle imaging velocimetry [50], and previously employed to study syneresis in colloidal gels [51]. The magnitude of the displacement vector $\overline{X}_v$, displayed as a function of $\tilde{t}$ in Fig. 3(b), is taken as a metric of structural changes between two successive images (see Movie 2 within the SM [36]). When the suspension is liquid, $\overline{X}_v$ is constant and its value is attributed to random correlations between images. Beyond the gel point ($\tilde{t} > 3$), $\overline{X}_v$ drops abruptly, as the structure displacements slow down to eventually stop when the gel is fully formed. Finally, for $\tilde{t} > \tilde{t}_c = 10$, $\overline{X}_v$ is constant and the method does not detect any additional changes in the gel microstructure for length scales superior to 0.1 μm. The setting of microstructure at $\tilde{t}_c = 10$ is fully consistent with the change in the dynamics of $G_0(\tilde{t})$ and $\omega_0(\tilde{t})$ depicted in Figs. 2(c) and 2(d). Comparison of images taken at $\tilde{t} = 1$ and 10 [insets in Fig. 3(b)] shows the evolution of finely distributed clusters at $\tilde{t} = 0$ to a coarse network, consistent with the increase of the fractal dimension measured in USAXS.

Building on these observation, we can propose a microscopic scenario accounting for the two-step aging dynamics of enzymatic milk gels. The first step is dominated by a coarsening of the gel network that involves large-scale rearrangements of the microstructure. It leads to a fast increase of the gel elasticity G_0 up to the time $\tilde{t}_c = 10$, which corresponds to an arrest transition, and a "freezing" of the microstructure that ceases to rearrange. In Fig. 2(c), for $\tilde{t} > \tilde{t}_c$, we observe that, despite the lack of microscale rearrangements, the gel's elastic properties continue to strengthen, although at a slower pace, switching from $G_0 \sim \tilde{t}^{1.6}$ for $\tilde{t} < \tilde{t}_c$ to $G_0 \sim \tilde{t}^{1.1}$ for $\tilde{t} > \tilde{t}_c$. This observation suggests that mechanical aging is now driven by some local aging process. Here, we hypothesize that the macroscopic mechanical aging is due to contact-driven aging between neighboring casein micelles, as postulated in previous studies on enzymatic milk gels [29,31].

In fact, contact-driven aging dynamics has been previously reported in gels of hard colloids [14], and more recently in dense suspensions of silica particles [22], where a constitutive relation between the shear modulus and the yield stress was established by determining the sample mechanical properties at various ages [23]. In case of contact-aging, the yield stress of the sample is expected to scale with the square root of the shear modulus, i.e., $\sigma_y \propto \sqrt{G'}$ [23]. To test whether such a relation is valid in gels of casein micelles, we conducted strain sweep tests at various aging times (inset in Fig. 4). Each experiments performed on a fresh gel yields an elastic modulus (at low strain values) and a yield stress σ_y determined by the abrupt drop in G' (see the SM [36]). At short aging times ($\tilde{t} < \tilde{t}_c$), σ_y vs G' increases exponentially, whereas for
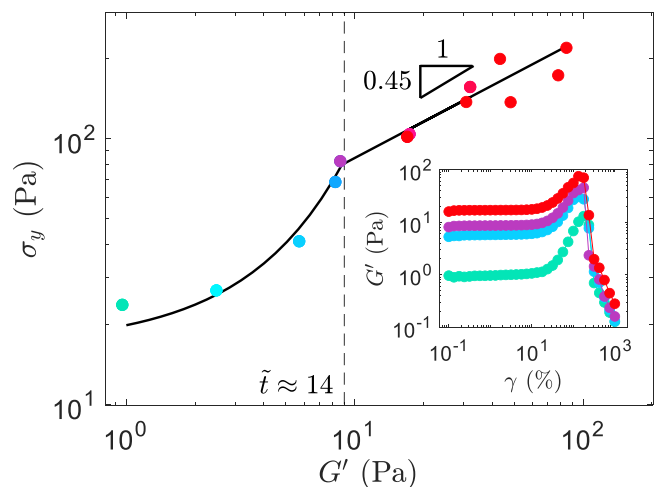

FIG. 4. Yield stress σ_y vs elastic modulus G' measured at different ages. Colors code for the aging time as in Fig. 1. Solid lines represent the best exponential and power-law fits of the data before and after $\tilde{t} \approx 14$, respectively. Inset displays strain sweep tests used to determine σ_y. From bottom to top $\tilde{t} = 5$, 11, 19, and 35.

$\tilde{t} \geqslant \tilde{t}_c$, we find that $\sigma_y \propto G'^{\lambda}$ with $\lambda = 0.45 \pm 0.05$ (Fig. 4), in very good agreement with the square-root prediction expected for contact-driven aging [23]. This result confirms that once the microstructure structure of enzymatic milk gel is frozen, the strengthening of the macroscopic mechanical properties of the gel proceeds through contact-driven aging.

Let us now summarize and discuss the key findings of this Letter. Using a multiscale approach, we have shown that the aging of enzymatic milk gels displays two distinct dynamics. The first regime is dominated by structural rearrangements so that the network formed at the gel point coarsens, without losing its fractal nature. We can further relate the fractal dimension of network and its power-law rheology, characterized by a single exponent Δ, using Muthukumar's relation [52]. The relation follows $\Delta = 3(d + 2 - 2d_f)/2(d + 2 - d_f)$, with d the euclidean dimension. Testing this relation with the exponents reported above for the critical gel ($\Delta = \beta = 0.62$) and the mature gel ($\Delta = \alpha = 0.28$) leads, respectively, to $d_f \approx 1.9$ at the gel point, and $d_f \approx 2.2$ for the mature gel, in good agreement with the values extracted from USAXS [Fig. 3(a)]. It demonstrates that structural rearrangements directly account for the evolution of the gel linear viscoelastic properties. This scenario contrasts with previous report on aluminosilicate and silica particle gels, where the structure of the network formed at the critical gel point was preserved during aging [35]. The preservation of the percolated network structure throughout aging is consistent with the framework developed by Adolf and Martins [34], where the time-connectivity superposition principle relies on the fact that aging essentially results in a change of scale. In the present case, despite the rearrangement of the structure formed at gel point, the time-connectivity principle still applies [Figs. 1(b) and 1(f)], highlighting its robustness, yet questioning its physical interpretation.

Following the coarsening of the network, the mesoscopic structure was found to "freeze" at a transition time $\tilde{t}_c = 10$. From this transition time, aging proceeds by contact aging

solely, as evidenced by the scaling of the yield stress with the square root of the elastic modulus. In this second regime, the elasticity of the gel increases linearly with $\tilde{t}$ [Fig. 2(c)], which is faster than the power-law increase $G' \sim t^{0.4}$ reported for silica particle gels showing contact aging [14]. It can be argued that contact aging between casein micelles probably starts immediately after aggregation, but does not preclude structural rearrangements. In fact, contact aging has been postulated as the motor of physical aging in enzymatic milk gels, as suggested by the sintering of casein micelles observed by electron microscopy [29,31]. Casein micelles are characterized by a Young modulus of about 10^5 Pa [53], and are significantly softer than colloidal particles usually employed to study colloidal gels (e.g., 10^{10} Pa for silica particles). More deformable particles were found to favor the local compaction of colloidal gels, due to a lower contribution of the bending mode to the stress relaxation [51,54]. Accordingly, local rearrangements of casein micelles due to contact aging may induce internal stresses in enzymatic milk gels, which is supported by their strong syneresis properties, as internal stresses are thought to be responsible for the pressure induced on the solvent during its expulsion [27,55].

Our results obtained through the prism of rheology strongly recalls the aging dynamics access using dynamic light scattering and X-ray correlation spectroscopy where the characteristic decorrelation time of the dispersion evolve with the aging time both in colloidal gels [18] and glasses [56,57]. In those studies, the two-step aging is associated with the softness of the particles and the presence of residual stresses. Specifically, in gels composed of soft latex colloids [18], sintering between the particles was also confirmed by electron microscopy, supporting the generality of our two-step aging scenario for a broad range of soft colloids.

Finaly, our results highlight three distinct time scales. The gelation time t_g and characteristic time τ enable rescaling of aging dynamics across a wide concentration range. Additionally, the value $\tilde{t} = 10$ indicates a clear separation in aging dynamics. We believe that the interplay between these time scales, along with the residual stresses in the gel network and the evolution of particle interactions over time, are key parameters for quantitatively modeling gel aging dynamics.

[1] T. Gibaud, N. Mahmoudi, J. Oberdisse, P. Lindner, J. S. Pedersen, C. L. P. Oliveira, A. Stradner, and P. Schurtenberger, Faraday Discuss. **158**, 267 (2012).

[2] Y. Cao and R. Mezzenga, Nat. Food **1**, 106 (2020).

[3] P. Bertsch, M. Diba, D. J. Mooney, and S. C. Leeuwenburgh, Chem. Rev. **123**, 834 (2023).

[4] K. Baskaran, M. Ali, K. Gingrich, D. L. Porter, S. Chong, B. J. Riley, C. W. Peak, S. E. Naleway, I. Zharov, and K. Carlson, Microporous Mesoporous Mater. **336**, 111874 (2022).

[5] V. Trappe and D. A. Weitz, Phys. Rev. Lett. **85**, 449 (2000).

[6] F. Cardinaux, T. Gibaud, A. Stradner, and P. Schurtenberger, Phys. Rev. Lett. **99**, 118301 (2007).

[7] E. Zaccarelli, J. Phys.: Condens. Matter **19**, 323101 (2007).

[8] L. C. Johnson, R. N. Zia, E. Moghimi, and G. Petekidis, J. Rheol. **63**, 583 (2019).

[9] T. Gibaud, T. Divoux, and S. Manneville, Nonlinear mechanics of colloidal gels: Creep, fatigue, and shear-induced yielding, in *Encyclopedia of Complexity and Systems Science*, edited by R.A. Meyers (Springer, Berlin, Heidelberg, 2020), pp. 1–24.

[10] W. H. W. Y. Shih, W. H. W. Y. Shih, S. I. Kim, J. Liu, and I. A. Aksay, Phys. Rev. A **42**, 4772 (1990).

[11] L.-V. Bouthier and T. Gibaud, J. Rheol. **67**, 621 (2023).

[12] M. Bantawa, B. Keshavarz, M. Geri, M. Bouzid, T. Divoux, G. H. McKinley, and E. Del Gado, Nat. Phys. **19**, 1178 (2023)

[13] J. H. Cho and I. Bischofberger, Phys. Rev. E **103**, 032609 (2021).

[14] S. Manley, B. Davidovitch, N. R. Davies, L. Cipelletti, A. E. Bailey, R. J. Christianson, U. Gasser, V. Prasad, P. N. Segre,

M. P. Doherty, S. Sankaran, A. L. Jankovsky, B. Shiley, J. Bowen, J. Eggers, C. Kurta, T. Lorik, and D. A. Weitz, Phys. Rev. Lett. **95**, 048302 (2005).

[15] G. Ovarlez and P. Coussot, Phys. Rev. E **76**, 011406 (2007).

[16] Y. M. Joshi, Annu. Rev. Chem. Biomol. Eng. **5**, 181 (2014).

[17] M. B. Gordon, C. J. Kloxin, and N. J. Wagner, J. Rheol. **61**, 23 (2017).

[18] L. Cipelletti, S. Manley, R. C. Ball, and D. A. Weitz, Phys. Rev. Lett. **84**, 2275 (2000).

[19] M. Bouzid, J. Colombo, L. V. Barbosa, and E. Del Gado, Nat. Commun. **8**, 15846 (2017).

[20] A. Jain, F. Schulz, I. Lokteva, L. Frenzel, G. Grübel, and F. Lehmkühler, Soft Matter **16**, 2864 (2020).

[21] N. Begam, A. Ragulskaya, A. Girelli, H. Rahmann, S. Chandran, F. Westermeier, M. Reiser, M. Sprung, F. Zhang, C. Gutt, and F. Schreiber, Phys. Rev. Lett. **126**, 098001 (2021).

[22] F. Bonacci, X. Chateau, E. M. Furst, J. Fusier, J. Goyon, and A. Lemaître, Nat. Mater. **19**, 775 (2020).

[23] F. Bonacci, X. Chateau, E. M. Furst, J. Goyon, and A. Lemaître, Phys. Rev. Lett. **128**, 018003 (2022).

[24] D. G. Dalgleish, Soft Matter **7**, 2265 (2011).

[25] C. G. De Kruif, T. Huppertz, V. S. Urban, and A. V. Petukhov, Adv. Colloid Interface Sci. **171-172**, 36 (2012).

[26] C. Holt, Eur. Biophys. J. **50**, 847 (2021).

[27] T. van Vliet, H. J. van Dijk, P. Zoon, and P. Walstra, Colloid Polym. Sci. **269**, 620 (1991).

[28] C. C. Fagan, D. J. O'Callaghan, M. J. Mateo, and P. Dejmek, *Cheese: Chemistry, Physics and Microbiology, Fourth Edition* (Academic Press, New York, 2017), Vol. 1, pp. 145–177.

[29] M. Mellema, P. Walstra, J. H. Van Opheusden, and T. Van Vliet, Adv. Colloid Interface Sci. **98**, 25 (2002).

[30] D. S. Horne and J. A. Lucey, *Cheese: Chemistry, Physics and Microbiology, Fourth Edition* (Academic Press, New York, 2017), Vol. 1, pp. 115–143.

[31] J. Bauland, M. H. Famelart, M. Faiveley, and T. Croguennec, Food Hydrocoll. **130**, 107739 (2022).

[32] H. H. Winter and F. Chambon, J. Rheol. **30**, 367 (1986).

[33] J. E. Martin, D. Adolf, and J. P. Wilcoxon, Phys. Rev. Lett. **61**, 2620 (1988).

[34] D. Adolf and J. E. Martin, Macromolecules **23**, 3700 (1990).

[35] B. Keshavarz, D. G. Rodrigues, J. B. Champenois, M. G. Frith, J. Ilavsky, M. Geri, T. Divoux, G. H. McKinley, and A. Poulesquen, Proc. Natl. Acad. Sci. USA **118**, e2022339118 (2021).

[36] See Supplemental Material at http://link.aps.org/supplemental/10.1103/PhysRevMaterials.8.L072601 for additional details about the sample preparation, the OWCh protocol, the yield stress measurements, the confocal microscopy experiments, the Ultra small-angle x-ray scattering experiments, and the effects of volume fraction on gelation and aging kinetics.

[37] M. Geri, B. Keshavarz, T. Divoux, C. Clasen, D. J. Curtis, and G. H. McKinley, Phys. Rev. X **8**, 041042 (2018).

[38] C. de Kruif, J. Dairy Sci. **81**, 3019 (1998).

[39] H. H. Winter and M. Mours, Rheology of polymers near liquid-solid transitions, in *Neutron Spin Echo Spectroscopy Viscoelasticity Rheology* (Springer, Berlin, 1997), pp. 165–234.

[40] T. H. Larsen and E. M. Furst, Phys. Rev. Lett. **100**, 146001 (2008).

[41] D. Chen, K. Chen, L. Hough, M. Islam, and A. Yodh, Macromolecules **43**, 2048 (2010).

[42] S. Costanzo, A. Banc, A. Louhichi, E. Chauveau, B. Wu, M. H. Morel, and L. Ramos, Macromolecules **53**, 9470 (2020).

[43] L. Morlet-Decarnin, T. Divoux, and S. Manneville, ACS Macro Lett. **12**, 1733 (2023).

[44] V. Adibnia and R. J. Hill, J. Rheol. **60**, 541 (2016).

[45] R. C. Koeller, J. Appl. Mech. **51**, 299 (1984).

[46] A. Bonfanti, J. L. Kaplan, G. Charras, and A. Kabla, Soft Matter **16**, 6002 (2020).

[47] A. Jaishankar and G. H. McKinley, Proc. R. Soc. A Math. Phys. Eng. Sci. **469**, 20120284 (2013).

[48] A. Bouchoux, G. Gésan-Guiziou, J. Pérez, and B. Cabane, Biophys. J. **99**, 3754 (2010).

[49] J. Teixeira, J. Appl. Crystallogr. **21**, 781 (1988).

[50] W. Thielicke and R. Sonntag, J. Open Res. Softw. **9**, 12 (2021).

[51] Q. Wu, J. van der Gucht, and T. E. Kodger, Phys. Rev. Lett. **125**, 208004 (2020).

[52] M. Muthukumar, Macromolecules **22**, 4656 (1989).

[53] J. Bauland, A. Bouchoux, T. Croguennec, M. H. Famelart, and F. Guyomarc'h, Food Hydrocoll. **128**, 107577 (2022).

[54] A. Thiel, T. J. Atherton, P. T. Spicer, and R. W. Hartel, Soft Matter **16**, 5506 (2020).

[55] M. Leocmach, M. Nespoulous, S. Manneville, and T. Gibaud, Sci. Adv. **1**, e1500608 (2015).

[56] R. Angelini, L. Zulian, A. Fluerasu, A. Madsen, G. Ruocco, and B. Ruzicka, Soft Matter **9**, 10955 (2013).

[57] V. Nigro, B. Ruzicka, B. Ruta, F. Zontone, M. Bertoldo, E. Buratti, and R. Angelini, Macromolecules **53**, 1596 (2020).